

Synthesis, structural, spectroscopic characterization, and structural comparison of 3-hydroxybenzoate and nicotinamide/*N,N*-diethylnicotinamide mixed ligand complexes with Zn(II)

Dursun Ali Köse · Hacali Necefoğlu ·
Onur Şahin · Orhan Büyükgüngör

Received: 27 October 2011 / Accepted: 6 December 2011 / Published online: 15 December 2011
© Akadémiai Kiadó, Budapest, Hungary 2011

Abstract The mixed-ligand 3-hydroxybenzoic acid complex of Zn(II) with nicotinamide and *N,N*-diethylnicotinamide were synthesized and characterized (colorless single crystals, $[\text{Zn}(\text{3-hba})_2(\text{H}_2\text{O})_2(\text{na})_2]$ and $[\text{Zn}(\text{3-hba})_2(\text{H}_2\text{O})_2(\text{dena})_2]$). The chemical, FT-IR, thermal, mass spectral analyses, and X-ray data results revealed that both of the compounds contain two water molecules, two 3-hydroxybenzoate (3-hba) and two nicotinamide (na) or two *N,N*-diethylnicotinamide (dena) ligands per formula unit. 3-hba and na or dena ligands bind to the Zn(II) ion monodentately through their acidic oxygen and pyridinic nitrogen atoms, respectively. The coordination of metal atoms are completed by two molecules of aqua ligands. The charge balance of complexes is accommodated by two molecules of 3-hba ions. The unit cell has two molecules coordination molecules and each of them was as settled to four surfaces of unit cell cage in na complex. There is one mole molecule that was occupied to center of unit cell cage in dena complex. The two dimensional network structure of the complex is like a hexagonal for na and square plane for dena complexes. The thermal decomposition takes place in three steps; first, dehydration of the two aqua ligands, second, elimination of the two nicotinamide ligands, finally, burning of the two benzoate ion ligands.

Keywords Mixed ligand complexes · Thermal decomposition · Zn(II) complexes · Crystal structure · Nicotinamide · *N,N*-diethylnicotinamide · 3-hydroxybenzoate

Introduction

Aromatic carboxylic acids are widely used in medicine as non-steroidal anti-inflammatory drugs (e.g., ibuprofen, naproxen, diclophenac, and fenclofenac) [1–4]. Phenolic antioxidants such as hydroxybenzoates are important classes of natural antioxidants [5]. 3-hydroxybenzoic acid is widely used as antimicrobial agents in foods, drugs, cosmetics, and toiletries [6]. Benzoic acid is used in combination with salicylic acid in dermatology as a fungicidal treatment (Whitfield's ointment) or fungal skin diseases (ringworm) [7]. It can be found in cosmetics, deodorants, and toothpastes [8, 9].

More widespread is the use of benzoic acid and its salts to preserve food from growth of microorganisms and it can be found in beverages, fruit products, chemically leavened baked goods, condiments as well as in the drink industry [10–12].

At the sametime Zinc element is known to regulate activity over 300 metalloenzymes and it is a component of special proteins, called “Zinc fingers” which participate in the reliable transfer of genetic information [13–15]. Zinc and its compounds have antibacterial and anti-viral activity and the wound-healing effect of Zinc-containing ointments has been known for several centuries [16–18]. Zinc may be used as a therapeutic agent, it may act as an anti-sickling agent and play a role in the prevention of pain crisis in sickle-cell disease. Zinc was successfully used in the treatment of acrodermatitis enteropathica, Wilson's disease, gastrointestinal disorders, infertility, and other diseases.

D. A. Köse (✉)
Department of Chemistry, Faculty of Arts and Sciences,
Hitit University, 19000 Çorum, Turkey
e-mail: dkose@hacettepe.edu.tr

H. Necefoğlu
Department of Chemistry, Faculty of Arts and Sciences,
Kafkas University, 36100 Kars, Turkey

O. Şahin · O. Büyükgüngör
Department of Physics, Faculty of Arts and Sciences,
Ondokuz Mayıs University, 55139 Kurupelit, Samsun, Turkey

Complex of Zinc(II) acetate with erythromycin is used in clinical medicine for acne therapy [19–22].

Moreover, the anti-bacterial effect of some drugs could be enhanced when they are chelated to a metal. Therefore, for the preparation of effective anti-microbial species it is very important to gain knowledge about the structure and bonding relations of the complexes. It is known that metal complexes of biologically important ligands are sometimes more effective than the free ligands [2]. It is well documented that heterocyclic compounds play a significant role in many biological systems, especially *N*-donor ligand systems being a component of several vitamins and drugs [23–27]. Structural reports on metal (Zn^{2+}) nicotinamide complexes exist in [28–31].

Nicotinamide is known as a component of the vitamin B complex as well as a component of the coenzyme, nicotinamide adenine dinucleotide (NAD). It is documented that heterocyclic compounds play a significant role in many biological systems, especially *N*-donor ligand systems being a component of several vitamins, and drugs such as nicotinamide. Itself plays an important role in the metabolism of living cells and some of its metal complexes are biologically active as antibacterial or insulin-mimetic agents [35, 36]. *N,N*-diethylnicotinamide is a derivative of nicotinamide (vitamin B) used as exhalation agent in respiratory systems in medicine [37]. The presence of the pyridine ring in numerous naturally abundant compounds, adducts of Dena are also of scientific interest. Therefore, these ligands had been the subject of many studies [38–41].

In this study, Zn(II) with 3-hydroxybenzoate (3-hba)—nicotinamide (na), and *N,N*-diethylnicotinamide (dena) complexes have been synthesized and single crystal X-ray diffraction studies, mass spectrum analysis, thermal decomposition results have been presented. The decomposition pathways of the investigated complexes are discussed in connection with the available spectroscopic data. The structure differences are correlated and discussed each other. The dena complex was studied before just structural properties with single crystal XRD [42].

Experimental

Materials and instrumentation

All chemicals used were analytical reagent products. $ZnSO_4 \cdot 5H_2O$, 3-hydroxybenzoic acid, nicotinamide, and

N,N-diethylnicotinamide (Fig. 1) were obtained from Merck (Darmstadt, Germany). Elemental analyses (C, H, N) were carried out by standard methods (Tubitak Marmara Research Center). IR spectra were recorded in the 4000–400 cm^{-1} region with a Perkin Elmer spectrum One FT-IR spectrophotometer using KBr pellets. Thermal analyses (TGA, DTA) were performed by the Shimadzu DTG-60H system, in dynamic nitrogen atmosphere (100 mL/min) at a heating rate of 10 °C/min, in platinum crucibles as sample vessel, using $\alpha-Al_2O_3$ as reference. Mass spectrum data was recorded Agilent Technologies 5973 spectrophotometer using DIP-MS method.

Preparation of Zn(II)-3-hba-na/dena complexes

In the first step, 3-hydroxybenzoic acid sodium salt was prepared. In the second step, metal 3-hydroxybenzoate salts were synthesized from Na(3-hba) salt. Finally, the solution of nicotinamide (2 mmol) in distilled water (30 mL) was added dropwise to a stirred solution of $Zn(3-hba)_2(H_2O)_n$ (1 mmol) in hot distilled water (50 mL). The resulting solution was allowed 15–17 days for crystallization at room temperature. The crystals formed were filtered and washed with cold water and acetone and dried in vacuo. The complex included dena was synthesized same method using dena ligand instead of na ligand.

Calc. for $C_{26}H_{26}N_4O_{10}Zn$: C, 50.32; H, 4.19; N, 9.03. Found: C, 51.02; H, 3.98; N, 9.16.

Calc. for $C_{34}H_{42}N_4O_{10}Zn$: C, 55.74; H, 5.74; N, 7.65. Found: C, 55.27; H, 6.18; N, 7.69.

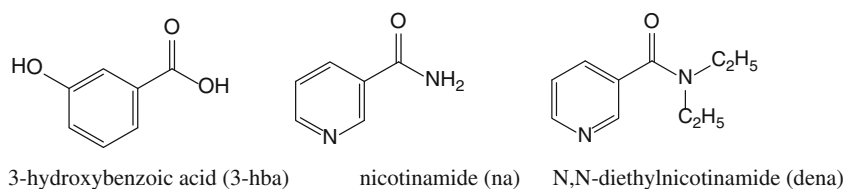
Results and discussion

According to analytical results per mole formula unit of complex contain two molecules of 3-hba–na or dena ligands and two mole aqua. It has not any hydrate aqua. The octahedral coordination of the metal ion is completed by two carboxylic oxygen atoms from two 3-hba and two nitrogen atoms from two na or dena and aqua oxygen atom.

FT-IR spectra

At the range of 3500–3000 cm^{-1} bands belong to asymmetric and symmetric stretching vibrations of aqua –OH groups. The bands for the N–H stretches of primary amides

Fig. 1 Molecule structure of ligands



in na complex were not seen clearly, so they had been concealed by –OH bands. Also N–H bending vibrations appear approximately in the range 1620 cm^{-1} . The 3-hba–na/dena mixed ligand complexes give rise to strong bands due to C=O stretching. It causes small frequency shifts conjugation between the carbonyl group and amide nitrogen. The observed strong bands at around 1575 cm^{-1} occurred at the same range as the amide group of free na/dena ligand that indicated the na/dena did not coordinate through amide group. Pyridine ring vibration of free na and dena at 1580 and 1560 cm^{-1} shifts to 1495 and 1480 cm^{-1} , respectively, in the complexes indicating that the pyridine ring is coordinated. The main difference in the spectrum of 3-hba is that the C=O stretching vibration of the carboxyl group at 1695 cm^{-1} shifts to lower frequency in all the metal complexes. The carboxylate bands in the metal complexes appear in the range of 1588 cm^{-1} for na and 1565 cm^{-1} for dena. This shows that the coordination takes place through the carboxyl group [27–29].

The –OH bending peak for the 3-hba remained almost in the same position at around 1270 cm^{-1} in all metal complexes. The low intensity bands in the region of $600\text{--}400\text{ cm}^{-1}$ are attributed to M–N and M–O vibration [27–31]. Some important IR bands of complexes are given in Table 1.

The IR spectra of all products are similar with $(\text{COO}^-)_{\text{asym.}}$ bands at 1588 cm^{-1} for na complex and 1565 cm^{-1} for dena complex, $(\text{COO}^-)_{\text{sym.}}$ bands at 1395 cm^{-1} for na complex, 1381 cm^{-1} for dena complex. The shift (Δ) between the $\nu_{\text{asym.}}$ and $\nu_{\text{sym.}}$ bands of COO^- groups are almost identical for both complexes (193 and 184 cm^{-1} , respectively) and indicate monodentate carboxylate [29–34].

Table 1 A summary of the FT-IR spectral data of na and dena complexes

Groups	[Zn(3-hba) ₂ (H ₂ O) ₂ (na) ₂]	[Zn(3-hba) ₂ (H ₂ O) ₂ (dena) ₂]
$\nu(\text{--OH})_{\text{H}_2\text{O}}$, $\nu(\text{NH})$	3,500/3,000	3,500/3,050
$\nu(\text{C=O})_{\text{ester}}$	1,703	1,720
$\nu(\text{COO}^-)_{\text{as}}$	1,588	1,565
$\nu(\text{COO}^-)_{\text{s}}$	1,481	1,464
$\Delta\nu$	107	101
$\nu(\text{C--O--C})$	1,144	1,144
$\nu(\text{C--H})_{\text{CH}_3}$	1,399	1,390
$\nu(\text{C--N})_{\text{py}}$	1,495	1,480
$\nu(\text{C--N})_{\text{amid}}$	1,251	1,258
$\nu(\text{C=O})_{\text{amid}}$	1,629	1,620
$\nu(\text{C--H})_{\text{C}_2\text{H}_5}$	–	2,984
$\nu(\text{Me--N})$	564	570
$\nu(\text{Me--O})$	424	459

Thermal analysis

[Zn(3-hba)₂(H₂O)₂(na)₂]

The TG–DTG/DTA curves for the [Zn(3-hba)₂(H₂O)₂(na)₂] complex are given in Fig. 2a. The complex has not any moisture and hydrate water. The molecule structure is stable in N₂ atmosphere as thermal up to $100\text{ }^\circ\text{C}$. Further heating causes two molecules of water ligands are released at two steps by an accompanying endothermic effect with the DTA curves at 104 and $130\text{ }^\circ\text{C}$ (6.00/5.81%). The anhydrous complex begins to decompose with melting at $210\text{ }^\circ\text{C}$ (DTA curve). Two molecules of neutral ligands nicotinamide are removed from the structure with endothermic effect at two steps (40.56/39.36%) after than, two molecules of 3-hba ligands are broken and decomposed with firing by produced CO/CO₂ (43.35/44.20%). Afterwards the decomposed and broken steps finally ZnO occur in the reaction crucible (12.55/13.13%) and this thermal product was indicated with FT-IR. All of the experimental data are suitable with calculation data, respectively.

[Zn(3-hba)₂(H₂O)₂(dena)₂]

The thermal analysis curves of [Zn(3-hba)₂(H₂O)₂(dena)₂] was given in Fig. 2b. According to thermal curves the complex decomposes four steps. The first step begin at $80\text{ }^\circ\text{C}$ and finish $130\text{ }^\circ\text{C}$ that belongs to removing of two molecules of aqua ligands (5.00/4.92%). There is not any other decomposing peaks in this area or before so we can say the structure has not got any moisture and hydrate water. The second step includes decomposing of four molecules of ethyl group of neutral ligand dena (17.55/15.85%). At the third step is attributed to decompose of pyridine rings of dena ligands (32.25/33.33%). All of the neutral ligands of complex remove in this step. The last step is composed of decomposing and removing of anionic ligands that it begins at $303\text{ }^\circ\text{C}$ and finish $380\text{ }^\circ\text{C}$ (38.45/37.41%). There are two endothermic DTA peaks between $320\text{ }^\circ\text{C}$ and $350\text{ }^\circ\text{C}$. After that step there is not any thermal decomposing action. Afterwards the decomposed and broken steps finally ZnO occur in the reaction crucible (12.05/11.12%) and this thermal product was indicated with FT-IR. All of the experimental data are suitable with calculation data, respectively.

Mass spectra

To deduce the thermal decomposition pathway for na and dena complexes mass spectrum were recorded (Figs. 3 and 4, respectively) using direct insertion probe pyrolysis mass spectrometry method. The molecular ion peak was detected at 617 for na and 727 for dena complex in the mass

Fig. 2 TG–DTG/DTA curves of the **a** $[\text{Zn}(\text{3-hba})_2(\text{H}_2\text{O})_2(\text{na})_2]$ and **b** $[\text{Zn}(\text{3-hba})_2(\text{H}_2\text{O})_2(\text{dena})_2]$ complexes

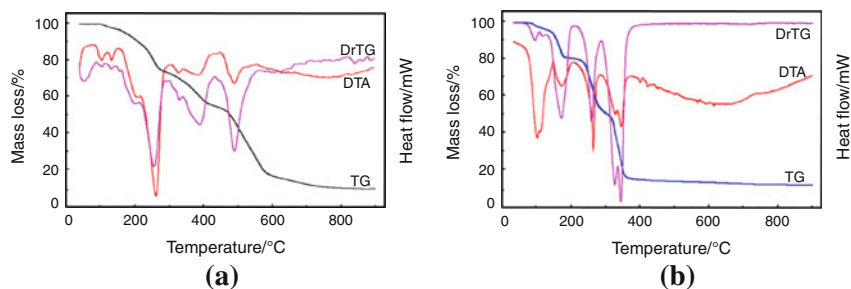


Fig. 3 Mass spectra of the $[\text{Zn}(\text{3-hba})_2(\text{H}_2\text{O})_2(\text{na})_2]$ complex

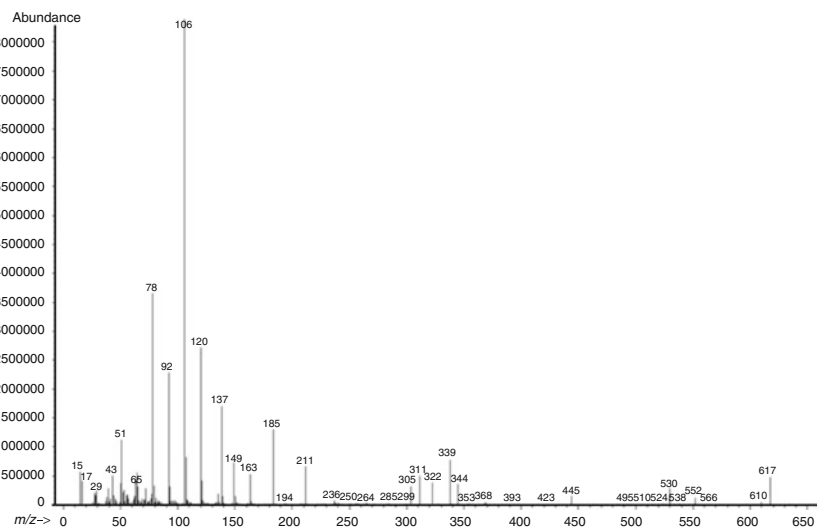
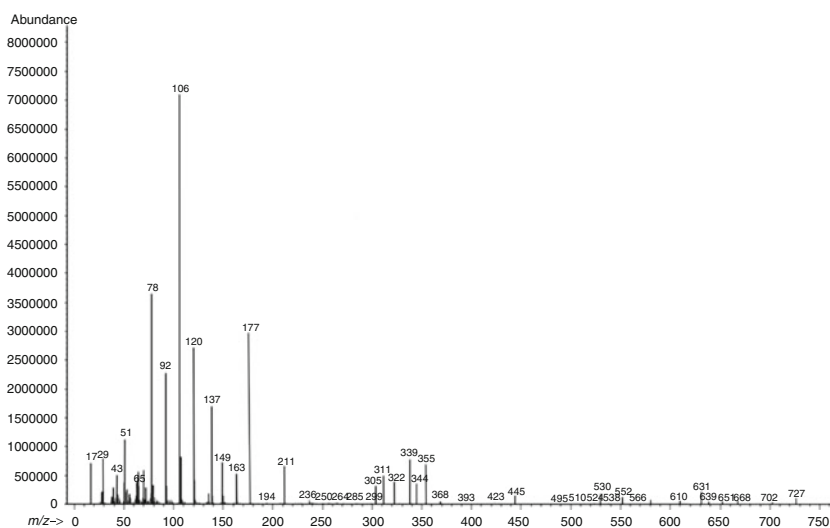


Fig. 4 Mass spectra of the $[\text{Zn}(\text{3-hba})_2(\text{H}_2\text{O})_2(\text{dena})_2]$ complex



spectrum recorded. The obtained pattern is relatively complex and exhibits a large number of peaks that belonging to the decomposition products of the complex and ligands. The decomposition peaks of na and dena complexes are harmonic with probable molecular ion peaks of decomposition products. The observed differences between na and dena complexes are just based on -ethyl groups dena. A schematic representation including the main fragmentation process for the $[\text{Zn}(\text{3-hba})_2(\text{H}_2\text{O})_2(\text{dena})_2]$ complex and ligands is given

in Scheme 1 and the main fragmentation process for $[\text{Zn}(\text{3-hba})_2(\text{H}_2\text{O})_2(\text{na})_2]$ is parallel to dena complex.

Crystal structure determination

The molecular structure and the atom-labeling scheme of na and dena complexes are shown in Fig. 5a, b. A colorless single crystal of the title compounds, $[\text{Zn}(\text{3-hba})_2(\text{H}_2\text{O})_2(\text{na})_2]$ and $[\text{Zn}(\text{3-hba})_2(\text{H}_2\text{O})_2(\text{dena})_2]$, suitable for data

Scheme 1 Mass spectral fragmentation pattern of the $[\text{Zn}(3\text{-hba})_2(\text{H}_2\text{O})_2(\text{dena})_2]$

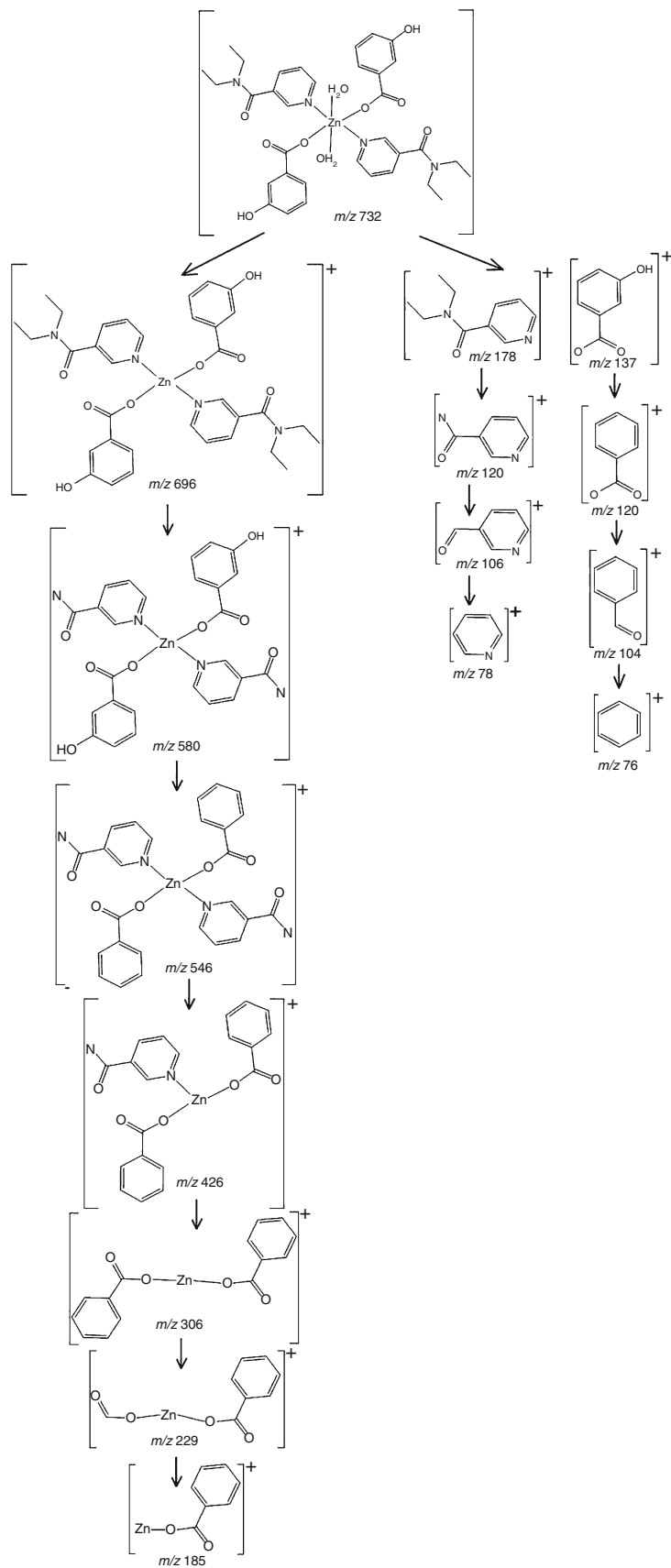


Fig. 5 Ortep of the molecules **a** for na and **b** for dena complexes with thermal ellipsoids drawn at 30% probability

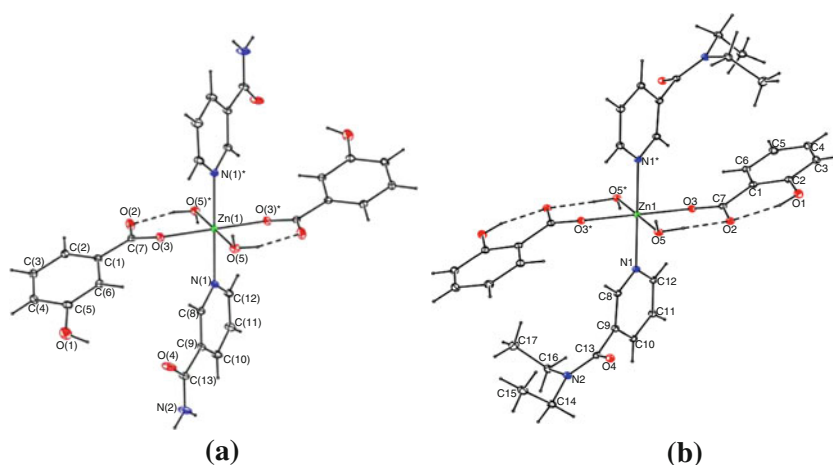


Table 2 Crystal data and refinement parameters for compounds

Empirical formula	[Zn(3-hba) ₂ (H ₂ O) ₂ (na) ₂]	[Zn(3-hba) ₂ (H ₂ O) ₂ (dena) ₂]
Formula weight (g/mol)	619.88	732.09
Crystal size (mm)	0.47 × 0.45 × 0.40	0.34 × 0.20 × 0.11
Crystal system	Monoclinic	Triclinic
Crystal form, color	Prism, colorless	Block, colorless
Space group	<i>P</i> 2 ₁ / <i>c</i>	<i>P</i> 1
<i>a</i> (Å)	7.2058 (3)	7.5531 (7)
<i>b</i> (Å)	18.1843 (9)	8.7459 (9)
<i>c</i> (Å)	10.5946 (5)	14.5419 (13)
α (°)	90.00	97.581 (8)
β (°)	111.139 (3)	94.864 (7)
γ (°)	90.00	114.137 (7)
<i>V</i> (Å ³)	1294.82 (10)	858.69 (14)
<i>Z</i>	2	1
Calculated density (g/cm ³)	1.590	1.416
Radiation type	Mo <i>K</i> α	Mo <i>K</i> α
μ (Mo <i>K</i> α) (mm ⁻¹)	1.02	0.78
Temperature (K)	296	100
θ range for data collection (°)	2.2–26.5	2.6–28.1
Reflections measured	9,485	7,774
Absorption correction	Integration	Integration
<i>T</i> _{min}	0.598	0.664
<i>T</i> _{max}	0.686	0.950
Independent reflections	2,670	3,531
Observed reflection (<i>I</i> > 2 σ (<i>I</i>))	2,479	3,091
<i>R</i> _{int}	0.020	0.069
Final <i>R</i> * indices (<i>I</i> > 2 σ (<i>I</i>))	<i>R</i> = 0.043, <i>wR</i> = 0.129	<i>R</i> = 0.049, <i>wR</i> = 0.128
Goodness-of-fit on <i>F</i> ²	1.07	1.07
(Δ / σ) _{max}	0.001	0.001
Max/min $\Delta\rho$ (e/Å ³)	2.00 and -0.55	0.91 and -1.19

Table 3 Selected bond lengths (Å) and Bond angles (°) for na complex

Bond	Dist.	Bond	Dist.
C(7)/O(2)	1.254 (3)	C(13)/N(2)	1.319 (4)
C(7)/O(3)	1.255 (3)	N(1)/Zn(1)	2.130 (2)
C(12)/N(1)	1.337 (4)	O(3)/Zn(1)	2.1233 (18)
O(5)/Zn(1)	2.164 (2)		
Angle (°)		Angle (°)	
O(2)/C(7)/O(3)	124.0 (2)	O(3)/Zn(1)/N(1)	88.40 (8)
O(4)/C(13)/N(2)	121.8 (3)	C(7)/O(3)/Zn(1)	125.05 (17)
C(7)/O(3)/Zn(1)	125.05 (17)	O(3)/Zn(1)/O(5)	86.08 (8)
C(8)/N(1)/Zn(1)	120.82 (18)	N(1)/Zn(1)/O(5)	87.27 (9)

Table 4 Hydrogen bonds for compound na (Å and °)

D/H...A	D(D/H)	d(H...A)	d(D...A)	<(DHA)
O(1)/H(1)...O(2)	0.82	2.14	2.661 (4)	121.7
O(5)/H(5B)...O(2)	0.827 (18)	1.81 (2)	2.607 (3)	162 (5)
O(5)/H(5A)...O(4)	0.82 (4)	2.17 (3)	2.927 (4)	153 (4)
C(2)/H(2)...O(1)	0.93	2.44	3.269 (4)	148.9
C(4)/H(4)...O(2)	0.93	2.62	3.470 (4)	153
N(2)/H(2A)...O(4)	0.86	2.12	2.953 (4)	162.8

Symmetry codes: #1: *x* + 1, *y*, *z*; #2: *x* - 1, -*y* + 3/2, *z* - 1/2; #3: -*x* + 1, -*y* + 1, -*z*; #4: -*x* - 1, -*y* + 1, -*z* - 1; #5: *x* - 1, *y*, *z*; #6: -*x*, -*y* + 1, -*z*; #7: -*x*, 1 - *y*, -1 - *z*

Table 5 Hydrogen bonds for compound dena (Å and °)

D/H...A	d(D/H)	d(H...A)	d(D...A)	<(DHA)
O(1)/H(1)...O(2)	0.82	1.83	2.554 (3)	147
O(5)/H(5B)...O(2)	0.832 (18)	1.856 (18)	2.681 (3)	171 (4)
O(5)/H(5A)...O(4 ⁱ)	0.823 (18)	1.966 (19)	2.783 (3)	172 (4)
C(5)/H(5)...O(2 ⁱⁱ)	0.93	2.45	3.333 (4)	159
C(10)/H(10)...O(2 ⁱⁱⁱ)	0.93	2.53	3.448 (3)	170

Symmetry codes: (i) -*x* + 2, -*y* + 1, -*z* + 1; (ii) *x* - 1, *y*, *z*; (iii) -*x* + 2, -*y* + 2, -*z* + 1

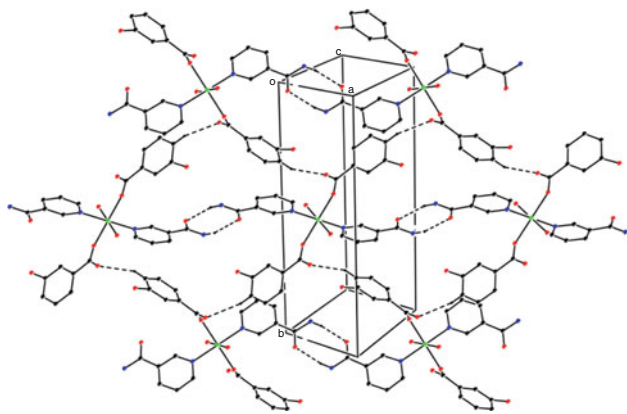


Fig. 6 Part of the crystal structure of na complex showing the formation of a chain rings along [101] generated by N–H...O and C–H...O hydrogen bonds

collection were mounted on a glass fiber and data collection was performed on a STOE IPDS II diffractometer with graphite monochromated MoK_α radiation at 296 and 100 K, respectively. Details of crystal data, data collection and refinement are given in Table 2. The structures were solved by direct-methods using SHELXS-97 and refined by full-matrix least-squares methods on F^2 using SHELXL-97

Fig. 7 The unit cell cage (a) and structure framework (b) of na complex

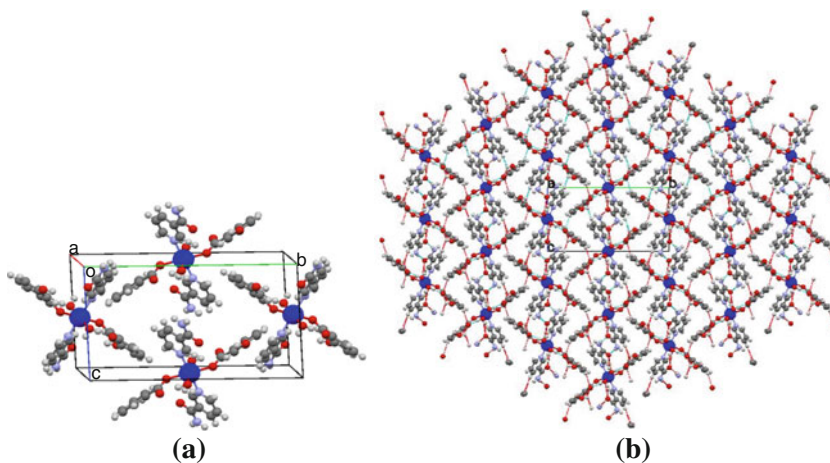
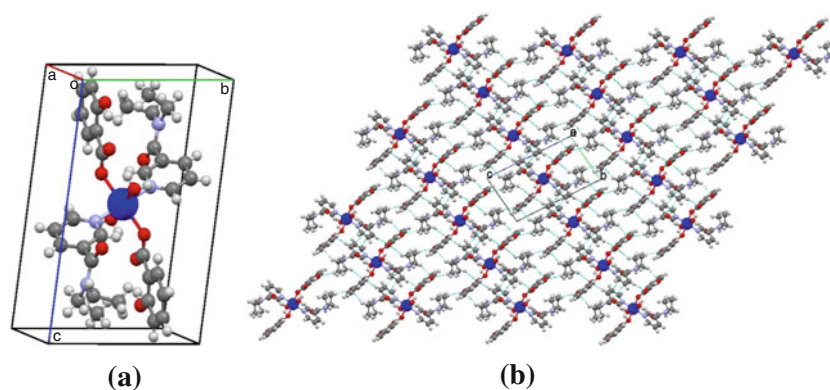


Fig. 8 The unit cell cage (a) and structure framework (b) of dena complex



[42] from within the WINGX [43] suitable of software. All non-hydrogen atoms were refined with anisotropic parameters. H atoms bonded to C and N atoms were included in their expected positions and allowed to ride, with C–H and N–H distances restrained to 0.93 and 0.86 Å, respectively, and with $U_{\text{iso}}(\text{H}) = 1.2 U_{\text{eq}}(\text{C}, \text{N})$. The H atoms of the hydroxy group was allowed for with a fixed O–H distance of 0.82 Å [$U_{\text{iso}}(\text{H}) = 1.5 U_{\text{eq}}(\text{O})$] in na complex. The H atoms of the water O atom were located in a Fourier difference map and freely refined.

The na and dena compounds crystallize in the space group $P2_1/c$ and $P1$ with $Z' = 1/2$ and 1, respectively. The Zn^{II} ion in na complex is located on a centre of symmetry and is coordinated by two O atoms from two equivalent carboxylate groups, two O atoms from aqua ligands, and two pyridyl N atoms. The geometry around the Zn^{II} ion (Table 2) is that of a distorted octahedron, the equatorial plane of which [O(3)/O(5)/O(3^{*})/O(5^{*})] is formed by two carboxylate O atoms [O(3) and O(3^{*})] and two aqua O atoms [O(5) and O(5^{*})] [symmetry code: (*) $1-x, 1-y, -z$]. The axial positions are occupied by two pyridyl N atoms [N(1) and N(1^{*})]. Carboxylate atom O(2) is pendant, with a longer Zn(1)...O(2) distance [3.289 Å] and larger Zn(1)–O(3)–C(7) angle consistent with the absence of

bonding between Zn(1) and O(2). The carboxylate group is not coplanar with the attached benzene ring, the dihedral angle between the planes being 16.26°. The pyridine and benzene rings are planar, the maximum deviations from the least-squares planes being 0.0050 Å for atom C(10) and 0.0127 Å for atom C(3).

Some selected bond distances and angles of na complex are given Table 3.

The hydrogen bonds of na and dena compounds are given Tables 4 and 5, respectively, that the reasons of structural differences can be seen easily in table data.

In the structure of na there is also a strong C–H... π interaction between C(10) (of a pyridine ring) atom in the molecule at (x, y, z) acts as a hydrogen-bond donor to the benzene ring C(1)–C(6) in the molecule at (–x, 1–y, –1–z), so forming a chain running parallel to the [101] direction. The details of the C–H... π interaction are given in Table 4. The combination of the C–H... π interactions define an $R_2^2(20)$ ring pattern (Fig. 6). The combination of the chains a long [100] and [101] suffices to generate a two-dimensional structure of considerable complexity.

There is more structural information about dena complex in literature [41].

The interesting framework structures and unit cell cages of molecules were shown in Figs. 7 and 8 for na and dena, respectively.

Conclusions

The na complex structure is octahedral like dena complex, but na complex unit cell structure is different from dena complex. While na complex is face centered type, dena complex is body centered according to Zn(II) metal ion. So their framework structures are very different. The framework structure of na complex like typically hexagonal, the dena complex framework like a square plane in 2D plane. There are two types H-bonding in dena complex between ethyl's H and O atoms of carboxylic acid. The unit cell molecules of this complex are bonded via these H-bonds. But na complex has lots of H-bonding type in establishment of molecular structure. Owing to lots of H-bonds na complex is very stable according to dena complex. The thermal decomposition results support this situation. All ligands are monodentate. According to thermal results; na complex is more stable than dena complex. The thermal decomposition of two studied structures begins by the release of aqua ligands. Dehydration of complexes begins at 80 °C for dena structure and 100 °C for na structure in one step. The stability of anhydrous complexes change as follows: na complex > dena complex. In the dena structure, decomposition of organic ligands begins with break off ethyl groups from dena molecules and then firstly,

neutral ligands (na and residue of dena) decompose and secondly ionic benzoate ligands remove from the structures. The Zinc(II)oxide remains to reaction vessel as last decomposition product.

According to mass analysis results both of the complexes disintegration patterns are similar to each other.

Supplementary material

CCDC-732372 contains the supplementary crystallographic data for this article. These data can be obtained free of charge from The Cambridge Crystallographic Data Centre via www.ccdc.cam.ac.uk/data_request/cif.

Acknowledgements The authors wish to acknowledge the Faculty of Arts and Sciences, Ondokuz Mayıs University, Turkey, for the use of the Stoe IPDS-II diffractometer (purchased from Grant No. F279 of the University Research Fund).

References

- Emery P, Kong SX, Ehrich EW, Watson DJ, Towheed TE. Dose-effect relationships of nonsteroidal anti-inflammatory drugs: a literature review. *Clin Ther.* 2002;24:1225–91.
- Sorenson JRJ. In: Sigel H, editor. *Metal ions in biological systems*. New York: Marcel Dekker; 1982.
- Dendrinou-Samara C, Tsotsou G, Ekateriniadou LV, Kortsaris AH, Raptopoulou CP, Terzis A, Kyriakidis DA, Kessissoglou DP. Anti-inflammatory drugs interacting with Zn(II), Cd(II) and Pt(II) metal ions. *J Inorg Biochem.* 1998;71:171–9.
- Stuhlmeier KM, Li H, Kao JJ. Ibuprofen: new explanation for an old phenomenon. *Biochem Pharmacol.* 1999;5:313–20.
- Rice-Evans CA, Miller NJ, Paganga G. Structure antioxidant-activity relationships of flavonoids and phenolic acids. *Free Radical Biol Med.* 1996;20:933–56.
- Hossaini A, Larsen JJ, Larsen JC. Lack of oestrogenic effects of food preservatives (parabens) in uterotrophic assays. *Food Chem Toxicol.* 2000;38(4):319–23.
- Diehl KB. Topical antifungal agents: an update. *Am Fam Physician.* 1996;54:1687–92.
- Rastogi SC, Lepoittevin JP, Johansen JD, Frosch PJ, Menne T, Bruze M, Dreier B, Andersen KE, White IR. Fragrances and other materials in deodorants: search for potentially sensitizing molecules using combined GC-MS and structure activity relationship (SAR) analysis. *Contact Dermatitis.* 1998;39:293–303.
- Sainio E, Kanerva L. Contact allergens in toothpastes and a review of their hypersensitivity. *Contact Dermatitis.* 1995;33: 100–5.
- Hanssen M, Marsden J. *The new E for additives*. Wellinborough: Thorsons Publishing, HarperCollins Publishers; 1987.
- Dock LL, Floros JD, Linton RH. Heat inactivation of *Escherichia coli* O157:H7 in apple cider containing malic acid, sodium benzoate and potassium sorbate. *J Food Prot.* 2000;63:1026–31.
- Islam M, Chen J, Doyle MP, Chinnan MS. Control of *Listeria monocytogenes* on turkey frankfurters by generally-recognized-as-safe preservatives. *J Food Prot.* 2002;65(9):1411–6.
- Vallee BL, Auld DS. Zinc coordination, function, and structure of zinc enzymes and other proteins. *Biochemistry.* 1990;29(24): 5647–59.

14. Kimura E, Koike T. Intrinsic properties of Zinc(II) ion pertinent to zinc enzymes. *Adv Inorg Chem*. 1997;44:229–61.
15. Kaim W, Schwederski B. *Bioinorganic chemistry: inorganic elements in the chemistry of life*. Chichester: Wiley; 1994.
16. Zelenak V, Sabo M, Massa W, Llewellyn P. Preparation, characterisation and crystal structure of two Zinc (II) benzoate complexes with pyridine-based ligands nicotinamide and methyl-3-pyridylcarbamate. *Inorg Chim Acta*. 2004;357:2049–59.
17. Korant BD, Kauer JC, Butterworth BF. Zinc ions inhibit replication of rhinoviruses. *Nature*. 1974;12(248–449):588–90.
18. De Clercq E. Antiviral metal complexes. *Metal-Based Drugs*. 1997;4:173–92.
19. Cunnane SC. *Zinc: clinical and biochemical significance*. Boca Raton: CRC Press; 1988.
20. Feucht CL, Allen BS, Chalker DK, Smith JG. Topical erythromycin with Zinc in acne. A double-blind controlled study. *J Am Acad Dermatol*. 1980;3:483–91.
21. van Hoogdalem EJ. Transdermal absorption of topical anti-acne agents in man; review of clinical pharmacokinetic data. *J Eur Acad Dermatol Venereol*. 1998;11:S13–9.
22. Kato M, Muto Y. Factors affecting the magnetic properties of dimeric Copper (II) complexes. *Coord Chem Rev*. 1988;92:45–83.
23. Nagar R. Syntheses, characterization, and microbial activity of some transition metal complexes involving potentially active O and N donor heterocyclic ligands. *J Inorg Biochem*. 1990;40(4):349–56.
24. Cavigiolio G, Benedetto L, Boccaleri E, Colangelo D, Viano I, Osella D. Pt (II) complexes with different N-donor aromatic ligands for specific inhibition of telomerase. *Inorg Chim Acta*. 2000;305:61–8.
25. Brühlmann U, Hayon E. One-electron redox reactions of water-soluble vitamins. I. Nicotinamide (vitamin B5) and related compounds. *J Am Chem Soc*. 1974;96(19):6169–75.
26. Köse DA, Gökçe G, Gökçe S, Uzun I. Bis(n,n-diethylnicotinamide)p-chlorobenzoate complexes of Ni(II), Zn(II) and Cd(II) synthesis and characterization. *J Therm Anal Calorim*. 2009;95(1):247–51.
27. Köse DA, Necefoglu H, Icbudak H. Synthesis and characterization of N,N diethylnicotinamide-acetylsalicylato complexes of Co(II), Ni(II), Cu(II), and Zn(II). *J Coord Chem*. 2008;61(21):3508–15.
28. Köse DA, Necefoglu H. Synthesis and characterization of bis (nicotinamide)m-hydroxybenzoate complexes of Co(II), Ni(II), Cu(II) and Zn(II). *J Therm Anal Calorim*. 2008;93(2):509–14.
29. Sahin O, Buyukgungor O, Köse DA, Necefoglu H. trans-Diaquabis(3-hydroxybenzoato-kO1)bis(nicotinamide-kN1)copper(II). *Acta Cryst*. 2007;C63:m510–2.
30. Köse DA, Kaya A, Necefoglu H. Synthesis and characterization of bis(N,N-Diethylnicotinamide) m-hydroxybenzoate complexes of Co(II), Ni(II), Cu(II) and Zn(II). *Russ J Coord Chem*. 2007;33:422–7.
31. Motz C, Roth HP, Kirchgessner M. Influence of bis(acetylsalicylato)-diaquo-zinc(II)-complex and acetylsalicylic acid on several parameters of the zinc status in growing rats. *Trace Elem Electr*. 1995;12(1):1–6.
32. Rzaczyńska Z, Kula A, Sienkiewicz-Gromiuk J, Szybiak A. Synthesis, spectroscopic and thermal studies of 2,3-naphthalenedicarboxylates of rare earth elements. *J Therm Anal Calorim*. 2011;103:275–81.
33. Jabłonska-Wawrzycka A, Zienkiewicz M, Hodorowicz M, Rogala P, Barszcz B. Thermal behavior of manganese(II) complexes with pyridine-2,3-dicarboxylic acid Spectroscopic, X-ray, and magnetic studies. *J Therm Anal Calorim*. 2001. doi:10.1007/s10973-011-1971-1.
34. Barszcz B, Masternak J, Surga W. Thermal properties of Ca(II) and Cd(II) complexes of pyridinedicarboxylates. Correlation with crystal structures. *J Therm Anal Calorim*. 2010;101:633–9.
35. Devereux M, Curran M, McCann M, Casey RMT, McKee V. Manganese(II) salicylate complexes as H₂O₂ disproportionation catalysts: X-ray crystal structure of [Mn(Hsal)₂(bipy)]·H₂O (H₂sal = salicylic acid, bipy = 2,2'-bipyridine). *Polyhedron*. 1999;15:2029–33.
36. Köse DA. Synthesis and structural characterization of nicotinamide/diethylnicotinamide complexes with acetylsalicylates of Co(II), Ni(II), Cu(II) and Zn(II). M. Sc. Thesis; Kafkas University; Kars; 2000.
37. Köse DA, Zumreoglu-Karan B, Unaleroglu C, Sahin O, Buyukgungor O. Synthesis and characterization of transition metal-vitamin B13 complexes with a Co-vitamin. *J Coord Chem*. 2006;59(18):2125–33.
38. Köse DA, Icbudak H, Necefoglu H. Synthesis and characterization of the nicotinamide-acetylsalicylato complexes of Co(II), Ni(II), Cu(II) and Zn(II). *Hacettepe J Bio Chem*. 2007;35(2):123–8.
39. Köse DA, Necefoglu H, Sahin O, Buyukgungor O. Synthesis, spectral, thermal and structural study of monoaquabis(acetylsalicylato-kO)bis(nicotinamide-kN)copper(II). *J Chem Crystallogr*. 2011;41:297–305.
40. Hökelek T, Necefoglu H. Diaquabis(N,N-diethylnicotinamide-N)bis(2-hydroxybenzoato-O) cobalt(II). *Acta Cryst*. 1997;C53:187–9.
41. Necefoglu H, Clegg W, Scott AJ. Diaquabis(N,N-diethylnicotinamide)bis(2-hydroxybenzoato)zinc(II). *Acta Cryst*. 2001;E57:m462–4.
42. Sheldrick GM. A short history of SHELX. *Acta Cryst*. 2008;A64:112–4.
43. Farrugia LJ. WinGX suite for small-molecule single-crystal crystallography. *J Appl Cryst*. 1999;32:837–8.